VERIFICATION OF THERMAL PERFORMANCE PREDICTIONS OF PROTOTYPICAL MULTI-JET IMPINGEMENT HELIUM-COOLED DIVERTOR MODULE

J. D. Rader, B. H. Mills, D. L. Sadowski, M. Yoda, and S. I. Abdel-Khalik

G. W. Woodruff School of Mechanical Engineering, Georgia Institute of Technology, Atlanta, GA 30332-0405 USA
said.abdelkhalik@me.gatech.edu

An experimental investigation of the thermal performance of the He-Cooled Multi-Jet (HEMJ) modular divertor design developed by the Karlsruhe Research Center (FZK) was previously performed at Georgia Tech using air at Reynolds numbers (Re) spanning those at which the actual He-cooled divertor is to be operated. The electrically heated test section was constructed from a brass alloy with nearly the same thermal conductivity as the tungsten alloy from which the prototypical HEMJ is to be constructed. More recently, another experimental investigation was performed by the Georgia Tech group for a similar finger-type divertor module using both air and He as coolants. The results of these experiments suggest that, in addition to matching Re, dynamic similarity between the air and He experiments requires that a correction be made to account for the differences in the relative contributions of convection and conduction (through the divertor walls) to the overall heat removal rate by the module. This correction factor depends on the thermal conductivity ratio of the solid to the coolant.

This investigation is aimed at quantifying the correction factor necessary to achieve dynamic similarity for the HEMJ to account for changes in the coolant and solid thermal conductivities. Experiments have been conducted using two (one each brass and steel) HEMJ test modules cooled with air, Ar, or He. The test modules were directly heated using an oxy-acetylene torch achieving heat fluxes up to 3 MW/m^2. The results of these experiments, together with data obtained using the aforementioned air-cooled experiments at lower heat fluxes (<1 MW/m^2) were used to develop a generalized correlation for the Nusselt number which accounts for changes in Re, as well as the solid to coolant thermal conductivity ratio. The correlation can be used to predict the performance of the actual He-cooled divertor at prototypical operating conditions.

I. INTRODUCTION

Several gas-cooled divertor designs have been investigated as part of the ARIES research program including the He-cooled multi-jet[1] (HEMJ), the He-cooled flat plate[2] (HCFP), and the He-cooled modular design with integrated fin array[3] (HEMP). The purpose of these thermal-hydraulic and thermo-mechanical studies is to ensure that these designs can withstand the anticipated heat fluxes (~10 MW/m^2) when operating in a magnetic fusion energy power plant without exceeding temperature and stress limits dictated by material properties.

The research group at Georgia Tech has utilized dynamic similarity to evaluate the thermal-hydraulic performance of the proposed divertor designs by performing a large number of low-temperature, low-pressure experiments. In general, test sections duplicating the geometry of the prototypical design are constructed out of brass (instead of tungsten and tungsten alloys) and cooled with air (instead of He). The experiments are conducted at non-dimensional mass flow rates (Reynolds number, *Re*) that span the expected operating *Re* value. The test modules are heated either electrically or, more recently, by an oxy-acetylene torch. Heat transfer coefficients (HTCs) are determined from calculated incident heat flux values and measured temperature readings from thermocouples embedded in the test section, and used to determine non-dimensional Nusselt numbers (*Nu*). The measured pressure drop across the test section is used to calculate a non-dimensional pressure loss coefficient (K_L). By correlating *Nu* and K_L to *Re*, parametric design curves are constructed that describe the thermal-hydraulic behavior of the design at prototypical operating conditions. For a given coolant inlet temperature and pressure, and a specified maximum allowable temperature for the pressure boundary, the maximum allowable incident heat flux and the corresponding pumping power fraction are determined based solely upon thermal-hydraulics (*vs.* thermal stress) considerations.

II. THE HEMJ AND HEMP DIVERTORS

Most recently, two modular finger-type divertors, the HEMJ and HEMP, designed by Karlsruhe Research

Center (FZK), have been studied at Georgia Tech. The HEMJ divertor cools the inner surface of the divertor tiles using an array of twenty-five round jets (Fig. 1). Hot He enters the inner tube at ~600°C and 10 MPa, passes through the array of round jets thus cooling the inner surface of the endcap (i.e. the pressure boundary), thereby removing the incident heat flux on the divertor tiles, and exits at ~700 °C. The HEMJ is designed to accommodate 10 MW/m^2 incident heat flux while keeping the tungsten alloy endcap peak temperature below 1300°C.

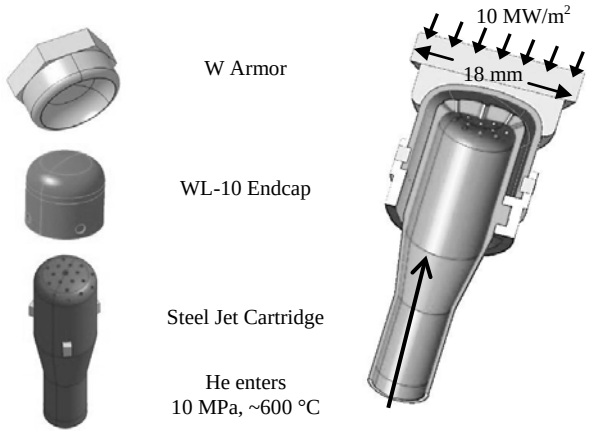

Fig. 1. The HEMJ divertor[10].

Previously, experimental research on the HEMJ was performed at Georgia Tech[4–6] using a brass test section electrically heated at heat fluxes up to 0.9 MW/m^2 cooled with air entering the test section at ~20 °C and ~700 kPa. Although these earlier experimental results were not extrapolated to prototypical conditions, numerical simulations using a model validated against the experimental results were used to predict the behavior of the brass HEMJ when tested at the HEBLO test facility at FZK near-prototypical pressures (8 MPa) at incident heat fluxes up to 5 MW/m^2.

Experiments[7,8] performed by FZK with the HEMJ using He at elevated inlet temperature (~600 °C) and pressure (~10 MPa) indicated that the HEMJ could withstand heat fluxes as great as 12 MW/m^2 at the nominal He mass flow rate (6.8 g/s). Further tests[9] on a bundle of nine HEMJ fingers at the Efremov Institute in Russia confirmed these results.

The HEMP (Fig. 2), in contrast, utilizes the heat transfer enhancement effect of an array of fins integral to the inner surface of the divertor pressure boundary instead of impinging jets. Hot He at ~600 °C and 10 MPa enters in an annular channel before flowing radially inward through the array of fins over the cooled surface and then exits axially through a central port at ~700°C. Fabricating the HEMP fin array in tungsten alloys has proven difficult[8] and thus experiments like those on the HEMJ at prototypical conditions have yet to be performed.

Earlier experimental and numerical studies on a HEMP-like divertor[11,12] predicted the performance of the HEMP under prototypical conditions. However, as described by Mills *et al.*[13], predicted prototypical divertor performance based on non-dimensional Nu and K_L values obtained from an air-cooled brass test module may not be accurate because these predictions do not account for the differences in the relative contributions of convection and conduction through the divertor walls.

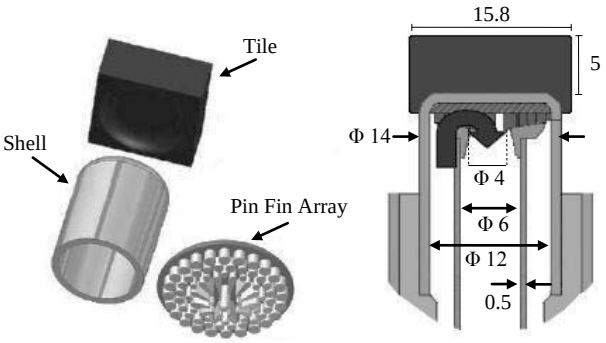

Fig. 2. Exploded view [left] and cross-section [right] of the HEMP divertor[11]. All dimensions in mm.

The previous experiments performed on an electrically heated HEMJ module cooled with air were therefore re-examined by accounting for the difference in the relative contributions of convection and conduction, characterized by the ratio of the thermal conductivities of the solid and the coolant, to the overall heat removal capability of the divertor module. To this end, additional experiments have been performed using two HEMJ test sections made of brass and steel, respectively, heated with an oxy-acetylene torch at incident heat fluxes up to 3 MW/m^2 and cooled by air, Ar, or He. By varying both the coolant and divertor thermal conductivities, these experiments at different thermal conductivity ratios are designed to verify that these experiments can, by accounting for this effect, give accurate predictions of the thermal performance of the HEMJ design at prototypical conditions.

III. EXPERIMENT

The torch-heated test sections are composed of two primary components: a jet cartridge, which creates round jets, concentric with and inside a thimble that simulates the pressure boundary. Two thimbles were machined, one of C36000 brass alloy and one of AISI 1010 carbon steel. Two jet cartridges were also machined, both out of C36000 brass. The jet cartridges have 24 0.6 mm diameter jets arranged in groups of six placed on four concentric circles with radii of 2.22 mm, 3.52 mm, 4.77 mm, and 6.49 mm projected to a plane at the top of the jet cartridge centered about one 1 mm diameter jet. The

thimble and the jet cartridge are separated by a 0.9 mm gap. Schematic drawings of the jet cartridge and thimble are shown in Fig. 3.

The volumetric flow rate of coolant into the test section is measured using a Brooks variable area flow meter (Model 1110) and used along with the density of the coolant calculated using temperature and pressure measurements from an OMEGA type E TC and OMEGA PX302-2KGV pressure transducer at the exit of the flow meter to determine the mass flow rate, $\dot{m}$. The temperature of the coolant was measured at the inlet, T_i, and outlet, T_o, of the test section by two OMEGA type E TCs and used to calculate the total incident power on the thimble, and hence, the average heat flux over the heated surface, $\overline{q''}$:

$$\overline{q''} = \frac{\dot{m}\overline{c_P}(T_o - T_i)}{A_h} \qquad (1)$$

where $\overline{c_P}$ is the constant pressure specific heat capacity of the coolant evaluated at the average of T_i and T_o, and A_h is the area of the heated surface, 227 mm^2.

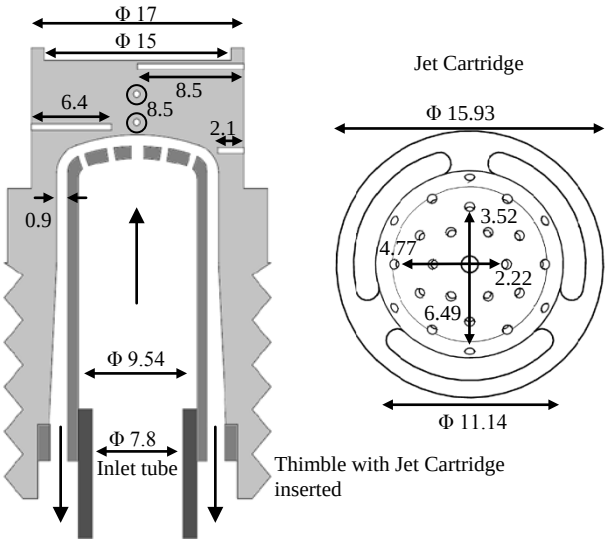

Fig. 3. Diametric cross-section of the HEMJ thimble and jet cartridge showing the locations of 5 of the 6 TCs [left] and top view of the jet cartridge showing the array of round jets [right]. The TCs in the center of the thimble (circled) are normal to the viewing plane and inserted 8.5 mm. The sixth TC, which is not shown here, is inserted 4.2 mm normal to this plane. Dimensions are in mm

The temperature distribution in the thimbles was measured using six 0.5 mm embedded type E OMEGA TCs (Fig. 3). The readings from the four TCs nearest the cooled surface spaced 90° apart and radially located 6.4, 4.3, 2.1, and 0 mm at axial locations 8.26, 6.88, 6.36, and 6.25 mm relative to the top of the thimble are used to determine the HTC. These TC readings are extrapolated through 0.5 mm of brass or steel to the cooled surface using $\overline{q''}$ assuming 1-D conduction. The extrapolated temperatures are then area averaged over the projected cooled surface area, A_c = 132 mm^2, resulting in an average cooled surface temperature, $\overline{T_c}$.

The pressure drop, across the divertor Δp was measured using an OMEGA PX26 differential pressure transducer. The inlet pressure was measured with an OMEGA PX302-300AV pressure transducer.

A total of seven experimental configurations were studied: the torch-heated brass thimble cooled with air, Ar, or He; the torch-heated steel thimble cooled with air, Ar, or He; and the electrically heated brass thimble cooled with air, from previous experiments[5,6]. Data from a total of 60 experiments are presented here.

IV. EXPERIMENTAL RESULTS

The area-averaged HTC, $\overline{h}$, was calculated from $\overline{q''}$, $\overline{T_c}$, T_i, and the area ratio A_h/A_c:

$$\overline{h} = \frac{\overline{q''}}{\overline{T_c} - T_i}\frac{A_h}{A_c} \qquad (2)$$

The above equation assumes that all of the power incident on the thimble is removed by convection at the cooled surface, i.e. it ignores conduction through the annular walls of the thimble. The area averaged Nu, $\overline{Nu}$, and the Re of the central jet, Re_j, were calculated as follows:

$$\overline{Nu} = \frac{\overline{h}D_i}{\overline{k}} \quad \text{and} \quad Re_j = \frac{\dot{m}D_i}{A_j\mu_i} \qquad (3a \,\&\, 3b)$$

where D_i is the diameter of the central jet (1 mm), $\overline{k}$ is the gas thermal conductivity based on the average of T_i and T_o, A_j is the total area of all 25 jets (7.57 mm^2), and μ_i is the dynamic viscosity of the coolant at T_i.

Fig. 4 presents $\overline{Nu}$ as a function of Re_j, for all seven experimental conditions. Experimental uncertainty for both $\overline{Nu}$ and Re_j was calculated using standard techniques[14] and ranges from 2%-12% for $\overline{Nu}$ and 1% - 3% for Re_j. The largest uncertainties for $\overline{Nu}$ are seen for the smallest values of T_o - T_i.

As shown in Fig. 4, the seven experimental data sets each follow their own trend instead of conforming to a global $\overline{Nu}$ relation based solely on Re_j. This means it is incorrect to assume that $\overline{Nu}$ can be predicted by just Re_j – more specifically that all of the heat incident on the divertor is removed by convection at the cooled surface [Eq. (2)]. Since the HEMJ and HEMP divertor are both 'finger-type' and share many general features, it's

reasonable to assume that their thermal performance can be generally characterized in the same manner. As shown in Figs. 1-3, the designs remove heat by both convection through the cooled surface and conduction down the walls of the divertor. Using a similar method presented in more detail in Ref. 13 regarding experimental and numerical studies on a HEMP-like divertor, an additional non-dimensional parameter k_s/k, or κ, was required to account for the change in conduction and convection heat removal rates at the cooled surface based on the different combinations of structure and coolant thermal conductivities.

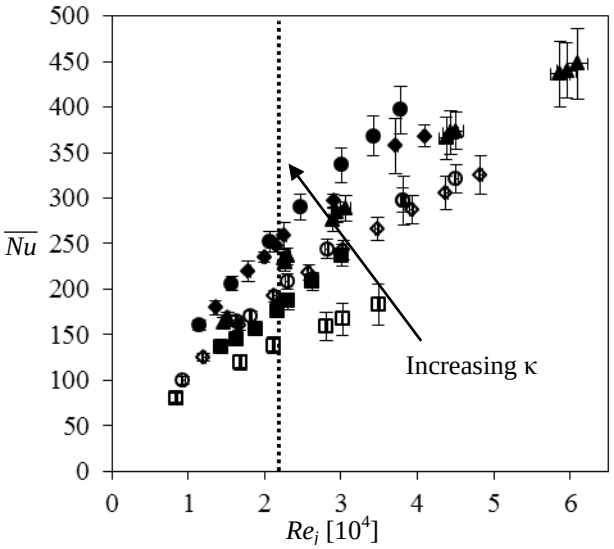

Fig. 4. $\overline{Nu}$ versus Re_j for all seven experimental configurations. Solid symbols for brass thimbles (air ♦, Ar ●, He ■, and electrically heated air▲) and open symbols for the steel thimble (air◊, Ar ○, and He □). Prototypical Re_j value of 21,600 shown with dotted line. Experimental uncertainty is indicated, though uncertainty in Re_j is almost unnoticeable at this scale for most cases.

As indicated on Fig. 4, the trends of $\overline{Nu}$ to Re_j are layered according to κ. By relating both Re_j and κ to $\overline{Nu}$, and assuming a power law correlation, each of the seven experimental data sets is now shown to follow a global trend (Fig. 5). Nearly all of the data points fit within the range of ±10% of the correlation as shown by the dashed lines. A dotted line indicates the prototypical operating point. The values of the fitting parameters are given by Eq. (4):

$$\overline{Nu} = 0.059 \cdot Re_j^{0.669} \kappa^{0.190} \tag{4}$$

The approximate value of κ for each experimental setup is shown in Table I and varies from ~370 for the He-cooled steel thimble experiments to ~7000 for the Ar-cooled brass thimble experiments. The prototypical value of κ is expected to be near 340. By covering a large range of both Re_j and κ, it is ensured that any extrapolation based on the experimental data is well characterized.

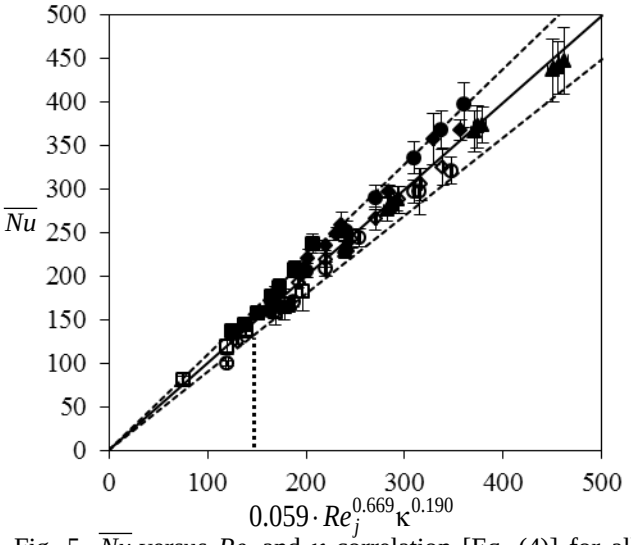

Fig. 5. $\overline{Nu}$ versus Re_j and κ correlation [Eq. (4)] for all experimental data shown with curve fit and ±10% dashed lines. Solid symbols for brass thimbles (air ♦, Ar ●, He ■, and electrically heated air▲) and open symbols for steel thimble (air ◊, Ar ○, and He □). Prototypical value of 140 (Re_j =21,600, κ =340) shown with dotted line.

TABLE I. Approx. values of κ for different conditions

Case	Approx. k_s [W/m-K]	Approx. k_g [W/m-K]	Approx. κ [-]
Ar Brass	135	0.018	7000
Air Brass	135	0.027	5000
Ar Steel	56	0.018	3000
Air Steel	56	0.027	2000
He Brass	135	0.16	850
He Steel	56	0.16	370
Prototypical	**115**	**0.33**	**340**

The pressure loss coefficient, K_L, was also calculated for each experiment and is plotted versus Re_j in Fig. 6. The density, ρ_L, and velocity, V_L, used in calculating K_L are determined using the outlet pressure and inlet temperature:

$$K_L = \frac{\Delta p}{\frac{1}{2}\rho_L V_L^2} \tag{5}$$

A curve fit assuming a power law plus a constant trend for K_L is given by Eq. (6):

$$K_L = 1.39 \cdot \left(Re_j / 10^4 \right)^{-0.50} + 1.32 \qquad (6)$$

Since K_L represents the "hydraulic" characteristics of the module, it is appropriately correlated by only matching Re_j (and geometry). The loss coefficients from the electrically heated experiments are not included as those experiments did not use an accurate differential pressure measurement technique.

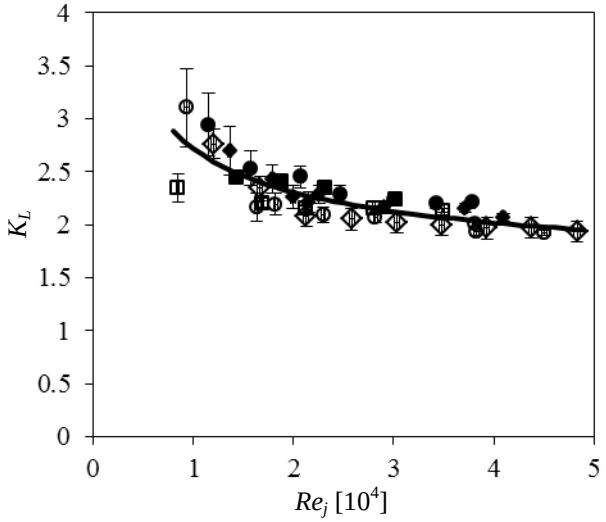

Fig. 6. K_L versus Re_j with associated curve fit. Solid symbols for brass thimbles (air ♦, Ar ●, and He ■) and open symbols for steel thimble (air ◊, Ar ○, and He □). Experimental uncertainty is indicated, though uncertainty in Re_j is almost unnoticeable at this scale.

V. PROTOTYPICAL CONDITIONS

Using the performance correlations in Eqs. (4) and (6), predictions of the behavior of the HEMJ at prototypical conditions (i.e. 10 MPa He inlet pressure, and 600 °C He inlet temperature) are made. Performance predictions are presented in terms of the average pressure boundary heated surface temperature, $\overline{T_s}$, the heat flux $\overline{q''}$, and the pumping power fraction β, i.e. the ratio between the pumping power and the incident thermal power:

$$\beta = \frac{\dot{m}\Delta p}{\bar{\rho}\overline{q''}A_h} \qquad (7)$$

where $\bar{\rho}$ is the average coolant density between the inlet and outlet.

Lines of constant $\overline{T_s}$ are constructed by calculating $\overline{q''}$ from $\overline{T_s}$ and Re_j, by way of Eqs. (1), (2-4). First a guess is made for T_o and $\overline{T_c}$ allowing for the calculation of κ and thus $\overline{Nu}$ by Eq. (4) and $\overline{h}$ by Eq. (3a). Then, a thermal resistance analogy for the conduction through the Δz = 1 mm pressure boundary allows for the calculation of $\overline{q''}$:

$$\overline{q''} = \frac{\overline{T_s} - T_i}{\frac{A_h}{A_c}\frac{1}{\overline{h}} + \frac{\Delta z}{k_s\left(\frac{\overline{T_s} + \overline{T_c}}{2}\right)}} \qquad (8)$$

where k_s is calculated based on the average of $\overline{T_c}$ and $\overline{T_s}$. This new value of $\overline{q''}$ gives new guesses for both T_o by Eq. (1) and $\overline{T_c}$ by Eq. (2). The process repeats until the values of T_o, $\overline{T_c}$, and $\overline{q''}$ converge.

Lines of constant β are calculated using Eqs. (5-7) as follows: as ρ_L and V_L depend on Δp, an iterative process is applied to Eq. (5) using K_L calculated with Eq. (6) from an assumed Re_j. With this value of Δp, $\overline{q''}$ is calculated based on a fixed value of β using Eq. (7). This also requires iteration since $\bar{\rho}$ depends on $\overline{q''}$.

As shown in Fig. 7, at the prototypical Re_j of 21,600, the HEMJ is predicted to withstand $\overline{q''}$ of ~14.1 MW/m^2 with $\overline{T_s}$ of 1200 °C while having a β value of ~8% based on a heated surface area of 227 mm^2. This corresponds to a heat flux of ~11.4 MW/m^2 for a hexagonal tile area of 280.6 mm^2 corresponding to a tile flat-to-flat distance of 18 mm (Fig. 1).

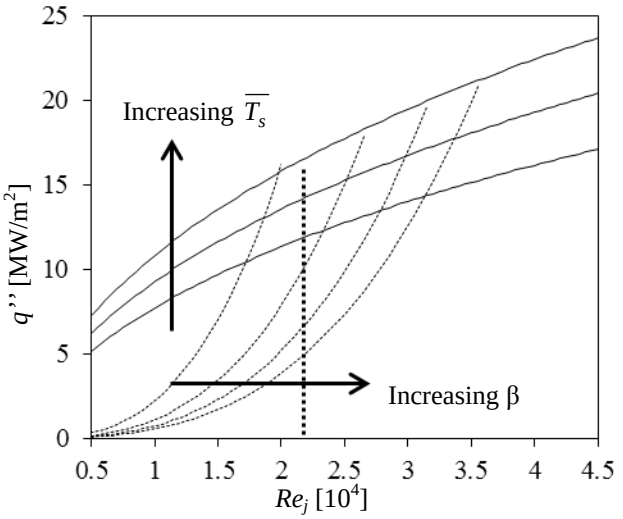

Fig. 7. Prototypical design curves for the HEMJ showing solid lines of constant $\overline{T_s}$ (1100°C, 1200°C, 1300°C) intersecting with dashed lines of constant β (5%, 10%, 15%, 20%). Prototypical Re_j = 21,600 indicated by vertical dotted line.

VI. CONCLUSIONS

As the HEMJ divertor design has been shown to withstand over 10 MW/m^2 incident heat flux at its nominal mass flow rate, an experimental investigation was undertaken to characterize the divertor's behavior under a wide range of operating conditions. These experiments used air, Ar, and He over a range of Re_j (8×10^3-6×10^4) and system pressure (0.6-1.4 MPa) to cool divertor test sections made of brass or steel and heated with an oxy-acetylene torch to heat fluxes ranging from 0.5-3 MW/m^2. Using nondimensional analysis and dynamic similarity, the results of these experiments were extrapolated to prototypical conditions (He cooling with inlet temperature of 600°C and pressure of 10 MPa) in order to produce performance curves. These curves allow magnetic fusion reactor designers to predict the HEMJ's behavior at normal and off-normal conditions with any variety of materials selection. Specifically, the maximum allowable incident heat flux can be determined for a given coolant flow rate (i.e. Reynolds number) and maximum allowable pressure boundary temperature. Values of the corresponding pumping power fraction are also given.

ACKNOWLEDGEMENTS

This work was performed as a part of the ARIES study. We thank the U.S. DOE Office of Fusion Energy Sciences for their support through contract number DE-FG02-01ER54656. We also recognize undergraduate researchers A. J. Polkinghorne and L. H. Stokes for their contributions to this research.

REFERENCES

1. T. IHLI, ET AL., "An advanced He-cooled divertor concept: Design, cooling technology, and thermohydraulic analyses with CFD," *Fusion Engineering and Design*, **75-79**, 371 (2005).
2. S. HERMSMEYER and S. MALANG, "Gas-cooled high performance divertor for a power plant," *Fusion Engineering and Design*, **61-62**, 197-202 (2002).
3. E. DIEGELE, ET AL., "Modular He-cooled divertor for power plant application," *Fusion Engineering and Design*, **66-68**, 383 (2003).
4. J. B. WEATHERS, ET AL., "Development of modular helium-cooled divertor for DEMO based on the multi-jet impingement (HEMJ) concept: Experimental validation of thermal performance," *Fusion Engineering and Design*, **83**, 1120 (2008).
5. J. B. WEATHERS, "Thermal Performance of Helium-Cooled Divertors for Magnetic Fusion Applications," *M.Sc. Thesis*, Georgia Institute of Technology (2007).
6. L. CROSATTI, "Experimental and Numerical Investigation of the Thermal Performance of Gas-Cooled Divertor Modules," *Ph.D. Thesis*, Georgia Institute of Technology (2008).
7. P. NORAJITRA, ET AL., "He-cooled divertor for DEMO: Experimental verification of the conceptual modular design," *Fusion Engineering and Design*, **81**, 341 (2006).
8. T. CHEVTOV, ET AL., "Status of He-cooled Divertor Development (PPCS Subtask TW4-TRP-001-D2)," P. NORAJITRA, Ed., Forschungszentrum Karlsruhe, Karlsruhe (2005).
9. P. NORAJITRA, ET AL., "Progress of He-cooled divertor development for DEMO," *Fusion Engineering and Design*, **86**, 1656 (2011).
10. T. IHLI, "He-cooled Divertor Development in the EU: The Helium Jet cooled Divertor HEMJ," *ARIES Meeting*, San Diego (2005).
11. B. H. MILLS, ET AL., "Experimental Investigation of Fin Enhancement for Gas-Cooled Divertor Concepts," *Fusion Science and Technology*, **60**, 190 (2011).
12. J. D. RADER, ET AL., "Experimental and Numerical Investigation of Thermal Performance of Gas-Cooled Jet-Impingement Finger-Type Divertor Concept," *Fusion Science and Technology*, **60**, 223 (2011).
13. B. H. MILLS, ET AL., "Dynamically similar studies of the thermal performance of helium-cooled finger-type divertors with and without fins," Accepted by *Fusion Science and Technology*.
14. S. KLINE and F. MCCLINTOCK, "Describing the uncertainties in single sample experiments," *Mechanical Engineering*, **75**, 3 (1953).